

# The Effects of Polysilastyrene and Au Additions on the Thermoelectric Properties of $\beta$ -SiC/Si Composites

H. NAKATSUGAWA,<sup>1,5</sup> K. NAGASAWA,<sup>1</sup> Y. OKAMOTO,<sup>2</sup> S. YAMAGUCHI,<sup>3</sup>  
S. FUKUDA,<sup>3</sup> and H. KITAGAWA<sup>4</sup>

1.—Yokohama National University, 79-5 Tokiwadai, Hodogaya-ku, Yokohama 240-8501, Japan. 2.—National Defense Academy, 1-10-20 Hashirimizu, Yokosuka 239-8686, Japan. 3.—Chubu University, 1200, Matsumoto-cho, Kasugai, Aichi 487-8501, Japan. 4.—Shimane University, Nishikawatsu 1060, Matsue, Shimane 690-8504, Japan. 5.—e-mail: naka@ynu.ac.jp

Recently, Yamaguchi et al. proposed a self-cooling device that does not require additional power circuits for cooling because it is Peltier-cooled using its own current in conjunction with a thermoelectric material. Silicon carbide is a promising thermoelectric material for this technology since its electrical conductivity, thermal conductivity, and Seebeck coefficient are higher than those of conventional thermoelectric materials. This study investigates the effects of polysilastyrene and Au additions on the thermoelectric properties of *p*-type  $\beta$ -SiC/Si polycrystalline semiconductor composites in order to assess whether their addition improves the performance of self-cooling devices.

**Key words:** Self-cooling device, Peltier cooling, silicon power device, silicon carbide, thermoelectric material

## INTRODUCTION

It is vital to cool silicon devices such as metal-oxide semiconductor field-effect transistors (MOSFETs), insulated gate bipolar transistors (IGBTs), and central processing units (CPUs) since they will not function correctly if they are operated at temperatures above 423 K. One way to remove heat from a silicon device is to use a conventional Peltier element, which is generally connected to a large fin and fan. The Peltier element and the fan require different DC power supplies, so that if a conventional Peltier element is used to cool a silicon device, the electric power consumption of the system will increase. This is one reason why conventional Peltier coolers are not used in laptop computers.

Recently, Yamaguchi et al.<sup>1,2</sup> proposed a self-cooling device for removing heat from silicon devices. This device does not require an additional power supply because Peltier cooling is achieved using the device's own current. Silicon carbide (SiC)<sup>1</sup> is a

promising material for this self-cooling device because its electrical conductivity, thermal conductivity, and Seebeck coefficient are higher than those of conventional thermoelectric materials. SiC is a wide bandgap semiconductor that is considered to be very promising for many applications. It is expected to be stable even at high temperatures because of its high chemical stability and mechanical hardness even at temperatures of around 1273 K.<sup>3</sup> However, the high thermal conductivity of SiC gives a low figure of merit  $Z = S^2\sigma/\kappa$  (where  $S$  is the Seebeck coefficient,  $\sigma$  is the electrical conductivity, and  $\kappa$  is the thermal conductivity). Many researchers have used SiC and conventional thermoelectric materials to control transport parameters by porosity control in various types of sintering methods.<sup>3-5</sup> To the best of the authors' knowledge, no research has yet been conducted to realize an advanced stage for thermoelectric materials. SiC has a large number of polytypes, including 3C, 4H, and 6H<sup>6-8</sup> (where the initial number indicates the number of Si-C bilayers in the unit cell and H and C, respectively, represent hexagonal and cubic crystal structures). In general, hexagonal and cubic SiC are known as  $\alpha$ - and  $\beta$ -SiC, respectively.

(Received August 1, 2008; accepted March 27, 2009)

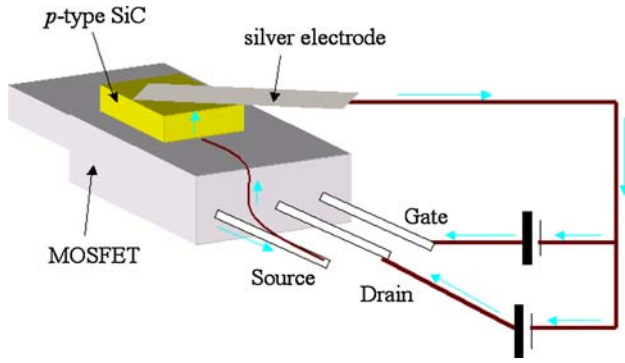


Fig. 1. Self-cooling device that consists of a power MOSFET and *p*-type SiC.

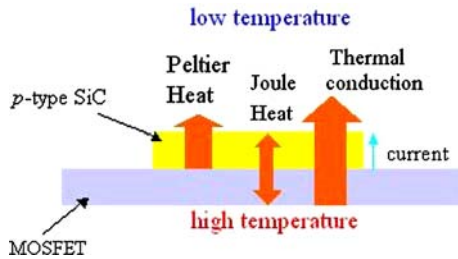


Fig. 2. Heat flux flow in the self-cooling device.

Figure 1 shows a schematic diagram of the self-cooling device. It consists of a vertical power MOSFET with *p*-type SiC, which is used to perform Peltier cooling. Its base is connected to the source of the MOSFET. Since the electric current is transferred from the drain to the source, both the electric current and the heat flux flow from the bottom to the top of the *p*-type SiC. Thus, the self-cooling device cools the power MOSFET. This differs from the conventional Peltier cooling process in which the Peltier element uses the Peltier heat as a heat pump, transferring heat from the cool side to the hot side. For this reason, it is usually desirable for Peltier materials to have low thermal conductivities. Because it is cooling a hot object, Peltier heat flows in the opposite direction in the self-cooling device to that in a conventional Peltier element (Fig. 2).

For a power device that has a thermoelectric element in its circuit, Peltier heat can increase the cooling efficiency to remove Joule heat from the device. Since Peltier heat is proportional to the current, more effective Peltier cooling can be achieved by using the device's own current in high-current power devices. In this system, Joule heat is generated isotropically and thermal conducted heat is transported upward by the Peltier effect from the power MOSFET. Since SiC has a high electrical conductivity, thermal conductivity, and Seebeck coefficient, it is a highly suitable material for the self-cooling device.

In this study, we investigated the effect of adding polysilastyrene (PSS, a sintering additive) and Au to

$\beta$ -SiC/Si composites on the thermoelectric properties of the composites. The purpose of this study is to investigate the thermoelectric properties and crystal structures of SiC/Si/Au composites in order to assess their suitability for use in the self-cooling device.

## EXPERIMENTAL PROCEDURE

Polycrystalline samples were prepared under the following conditions by a conventional solid-state reaction.  $\beta$ -SiC (average particle size 0.15  $\mu\text{m}$ , Mitsui Toatsu, 99.7%, MSC-20), Si (Kojundo Chemical Laboratory, 99.99%), and Au (150- $\mu\text{m}$  pass, Kojundo Chemical Laboratory, 99.9%) powder were used as the starting materials, and PSS (Nippon Soda, PSS-100) was mixed in as a sintering aid. Any excess PSS thermally decomposes and its components evaporate during sintering, producing pores in the sample. Slurries were made from mixed powders of (i) 60 wt.% SiC and 40 wt.% Si (SiC/Si = 60/40), (ii) 60 wt.% SiC and 40 wt.% Si and 10 wt.% PSS (SiC/Si = 60/40 + PSS), and (iii) 55 wt.% SiC, 40 wt.% Si, 5 wt.% Au and 10 wt.% PSS (SiC/Si/Au = 55/40/5 + PSS). The slurries were then mixed in polyethylene containers using nylon-coated iron balls as the grinding media and xylene solution as the mixing agent. These slurries were mixed for 24 h, passed through a 75-mesh sieve, and then dried. After drying the slurry, the powder obtained was granulated using a 500- $\mu\text{m}$ -mesh sieve.

The mixing powder was formed into pellets (20 mm  $\phi \times 5$  mm) by uniaxial pressing at  $1 \times 10^6$  kgf/m<sup>2</sup>. The pellets were then subjected to cold isostatic pressing (CIP; Nikkiso, CL3-22-60) at  $3.5 \times 10^7$  kgf/m<sup>2</sup> after being sealed in evacuated vinyl packing. During sintering, each pellet was crushed into the isocomposition powder. This powder was then placed in a carbon crucible, the internal surfaces of which had been coated with boron nitride. Sintering was conducted both in vacuum and in an atmosphere in a radiofrequency induction furnace (Fujidenpa, FVPHP-10) heated by graphite electrodes. First, the furnace was heated to 1273 K at a rate of 20 K/min in vacuum, and Ar gas then was introduced at atmospheric pressure. The furnace temperature was further raised to 2373 K at a rate of 10 K/min, and the sample was kept at this temperature for 2 h and then cooled naturally to room temperature. Finally, the furnace was cooled to 1873 K at a rate of 100 K/min and then naturally cooled to room temperature. The sintered bodies were cut into rectangular specimens of 2 mm  $\times$  10 mm  $\times$  10 mm in order to measure their thermoelectric properties and to assess their use in the self-cooling device.

The electrical resistivity and the Seebeck coefficient were measured in the temperature range of 80 K to 960 K. The electrical resistivity  $\rho$  was measured by the van der Pauw method with a

current of 10 mA in a He atmosphere (Toyo Corp, 8350LH/CD) at low temperatures (80 K to 400 K) and by a homemade device in an Ar atmosphere at high temperatures (300 K to 960 K). The Seebeck coefficient  $S$  was measured by placing a sample between two blocks of oxygen-free high-conductivity silver. The Hall coefficient  $R_H$  measurement was performed on flat square samples with a current of 100 mA in a magnetic field of 8500 Oe by the van der Pauw method at room temperature. The Hall carrier concentration  $n$  was determined from  $R_H$  using  $n = 1/eR_H$ , where  $e$  is the electron charge. Furthermore, the Hall mobility  $\mu$  was determined from  $\rho$  and  $R_H$  using  $\mu = R_H/\rho$ . The thermal diffusivity  $A$ , sample density  $D$ , and specific heat  $C$  were measured at room temperature, and the thermal conductivity  $\kappa$  was calculated using  $\kappa = ACD$ . The thermal diffusivity  $A$  was measured by the laser flash method using a thermal constant analyzer (TC-3000, ULVAC). The sample density  $D$  was measured by Archimedes' method using purified water as the solvent.

The microstructures of the samples were examined by a scanning electron microscope (SEM; VE-8800, Keyence) and the distributions of the elements Si, C, and Au in the microstructure after sintering were simultaneously determined using an electron-probe x-ray micro-analyzer (EPMA; JXA-8900R, JEOL). The chemical composition of Au, C and, Si in the sintered Au-doped SiC/Si samples was examined by using inductively coupled plasma (ICP) analysis, a direct combustion-gasometric method, and a gravimetric technique, respectively. The SiC content was calculated from the detected amount of carbon, and any residual silicon was ascribed to excess Si.

## RESULTS AND DISCUSSION

After sintering, an additional 10 wt.% to 20 wt.% Si and 2.5 wt.% Au were detected, compared with 40 wt.% Si and 5 wt.% Au before sintering; i.e., (i) SiC/Si = 90/10, (ii) SiC/Si = 80/20 + PSS, and (iii) SiC/Si/Au = 80/17/3 + PSS, respectively. This demonstrates that the amounts of these elements were reduced by more than 50%, even though the sintering temperature was below the boiling points of Si and Au.

The thermoelectric properties of the polycrystalline specimens of (i) SiC/Si = 90/10, (ii) SiC/Si = 80/20 + PSS, and (iii) SiC/Si/Au = 80/17/3 + PSS were measured in the temperature range from 80 K to 960 K. Figure 3 shows a discontinuous change at around 450 K and metallic behavior in the temperature range from 80 K to 450 K. In particular, sample (i) exhibits a broad maximum and a metal-semiconductor transition at around 600 K. Figure 4 shows the temperature dependence of the Seebeck coefficient  $S(T)$  of the samples in the temperature range from 80 K to 960 K. The Seebeck coefficient is clearly positive, which implies that the main

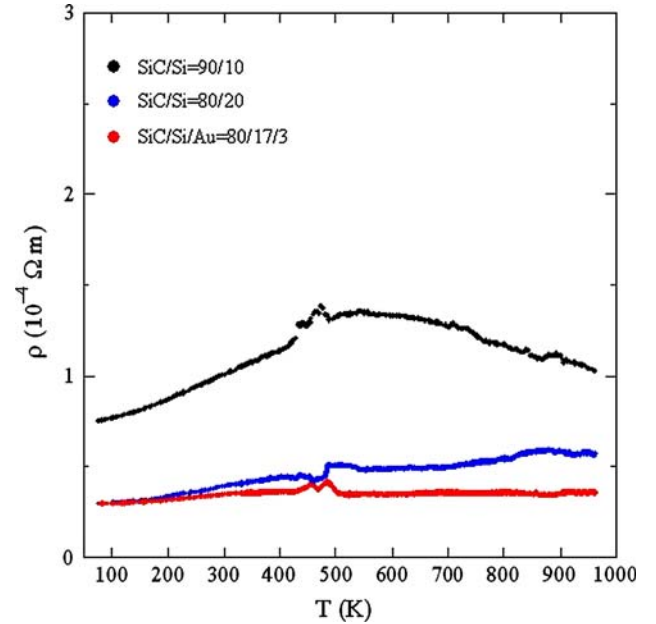


Fig. 3. Temperature dependence of electrical resistivity  $\rho$ .

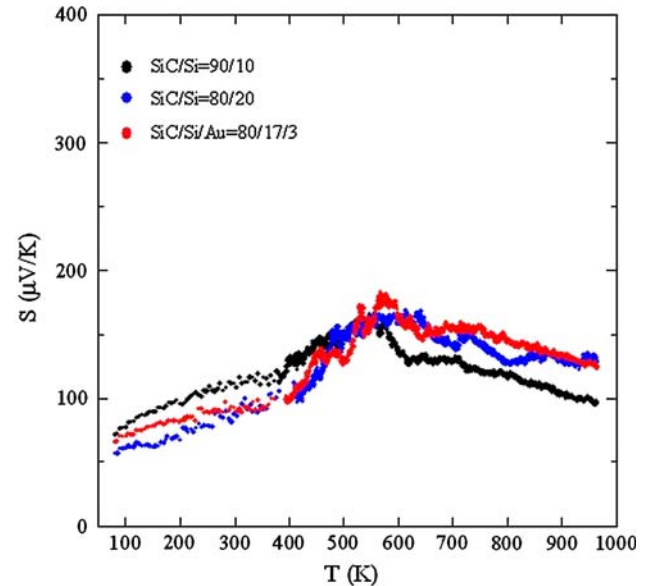


Fig. 4. Temperature dependence of Seebeck coefficient  $S$ .

carriers are holes. All the samples have a broad maximum at around 600 K; this maximum occurs at a lower temperature for sample (i) than for sample (iii).

Table I gives the measurement results for the thermoelectric properties of all the samples at room temperature. Of the three samples, sample (iii) has the smallest resistivity  $\rho$ , the largest power factor  $S^2/\rho$ , the largest hole mobility  $\mu$ , and the largest sample density  $A$ . The Seebeck coefficient  $S$  decreases and the thermal conduction  $\kappa$  increases as a function of PSS concentration, while  $S$  increases and  $\kappa$  decreases as a function of

**Table I. Electrical Resistivity  $\rho$ , Electrical Conductivity  $\sigma$ , Hall Coefficient  $R_H$ , Carrier Concentration  $n$ , Hole Mobility  $\mu$ , Seebeck Coefficient  $S$ , Power Factor  $S^2/\rho$ , Sample Density  $A$ , Thermal Diffusivity  $B$ , Specific Heat  $C$ , and Thermal Conductivity  $\kappa$  at Room Temperature**

	SiC/Si = 90/10	SiC/Si = 80/20	SiC/Si/Au = 80/17/3
$\rho$ ( $10^{-4}$ $\Omega$ m)	0.997	0.382	0.336
$\sigma$ ( $10^4$ $\Omega^{-1}$ m $^{-1}$ )	1.00	2.62	2.98
$S$ ( $10^{-6}$ V/K)	109	88.0	92.4
$S^2/\rho$ ( $10^{-8}$ W/m K $^2$ )	1.19	2.03	2.54
$R_H$ ( $10^{-8}$ m $^3$ /C)	3.09	1.99	1.93
$n$ ( $10^{26}$ /m $^3$ )	2.02	3.14	3.23
$\mu$ ( $10^{-4}$ m $^2$ /V s)	3.10	5.21	5.74
$A$ ( $10^3$ kg/m $^3$ )	1.69	2.10	2.17
$B$ ( $10^{-4}$ m $^2$ /s)	0.32	0.38	0.37
$C$ ( $10^{-3}$ J/kg K)	0.68	0.68	0.66
$\kappa$ (W/m K)	36.6	53.7	52.4

Au concentration. These results suggest that both samples (ii) and (iii) are promising materials for the self-cooling device.

Figure 5 shows SEM images of a cut surface of samples (i), (ii), and (iii). The grain size increases and the porosity decreases with the addition of PSS. Sample (i), which did not contain PSS, has a packing density of about 53%, while samples (ii) and (iii), to which PSS had been added, had packing densities of about 66% to 68%.

Figure 6 shows the time dependence of the average surface temperature distribution in the self-cooling device. As shown in Fig. 1, the self-cooling device consists of a commercial power MOSFET connected to sample (iii). Sample (iii), the base of which was connected to the source of MOSFET, achieved good Peltier cooling. Since the electric current (0.6 A) flows from the drain to the source when the voltage (8 V) is applied between the gate and the source, both the electric current and the heat flow from the bottom to the top of sample (iii). Figure 6 shows that the self-cooling device cools the power MOSFET. The static drain-to-source resistance of the commercial power MOSFET (FQPF3N90, Fairchild Semiconductor Corp.) is 3.3  $\Omega$ . Since the power MOSFET is continuously on and the current between the drain and the source is 0.6 A, about 1.19 W of Joule heating is generated. The Peltier heat flux on the bottom surface of sample (iii) after 150 s later is given by

$$Q_p = ST_H I = 92.4[\mu\text{V}/\text{K}] \times 350[\text{K}] \times 0.6[\text{A}] = 19[\text{mW}].$$

The thermal conduction from the bottom surface to the upper surface of sample (iii) is given by

$$\begin{aligned} K\Delta T &= 524[\text{mW}/\text{cm K}] \times 1[\text{cm}^2]/0.2[\text{cm}] \times 18[\text{K}] \\ &= 47.2[\text{W}], \end{aligned}$$

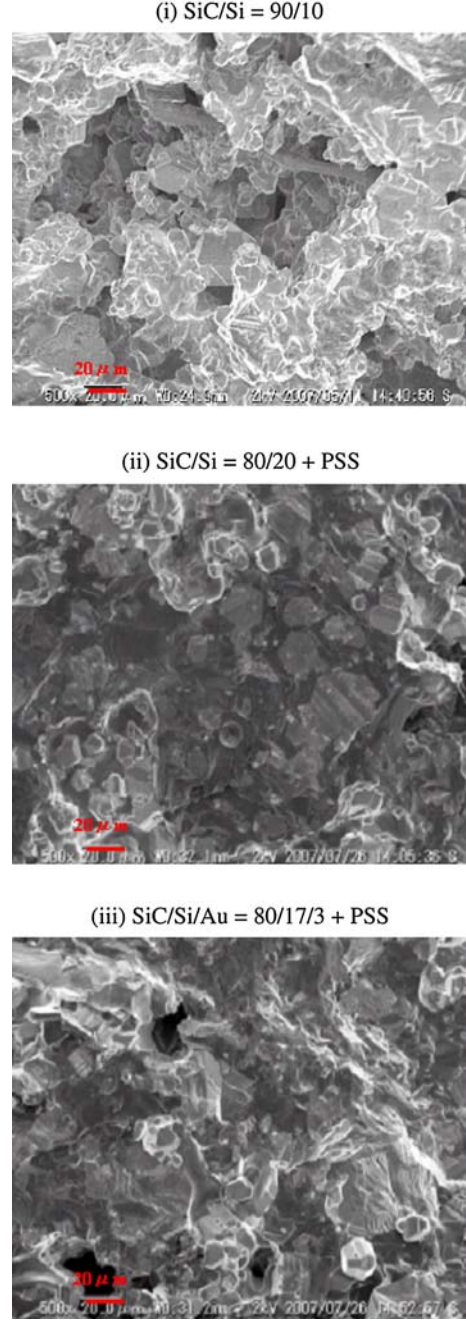


Fig. 5. SEM observations of cut surfaces of samples (i) SiC/Si = 90/10, (ii) SiC/Si = 80/20 + PSS, and (iii) SiC/Si/Au = 80/17/3 + PSS.

where  $K$  is the thermal conductance and  $\Delta T$  is the temperature difference between the bottom and upper surface of sample (iii) after 150 s. In this case, almost all the Joule heat generated in the power MOSFET is removed by Peltier cooling and thermal conduction.

## CONCLUSIONS

The thermoelectric properties of  $\beta$ -SiC/Si composites are improved by employing the sintering

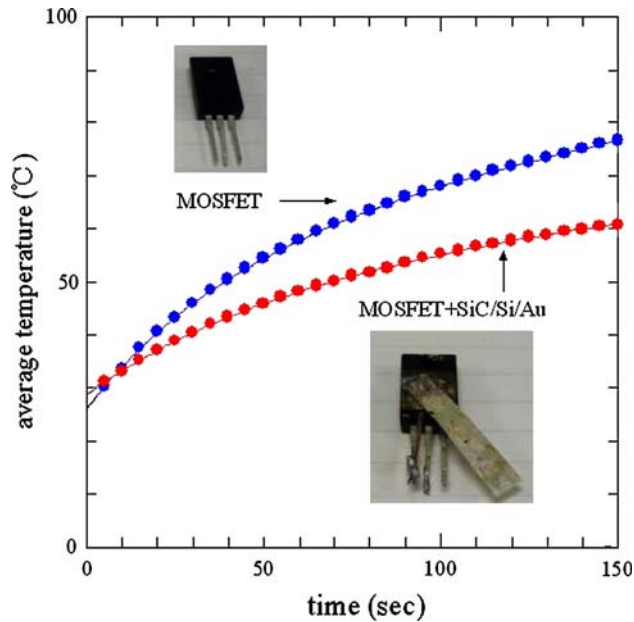


Fig. 6. Time dependence of the average surface temperature in MOSFET (blue circles) and MOSFET + (iii) SiC/Si/Au = 80/17/3 + PSS (red circles).

additive polysilastyrene. The grain size increases and the porosity decreases with the addition of PSS. As a result, the sample density, hole mobility, and thermal conductivity increase as a function of PSS concentration. The electrical resistivity at room temperature decreases by about 70% with the addition of PSS. The Seebeck coefficient at high temperature increases with the addition of PSS. The thermal conductivity at room temperature increases

with an increase in the PSS concentration, and is about 1.5 times larger than that of the sample without PSS. These results suggest that samples (ii) (SiC/Si = 80/20 + PSS) and (iii) (SiC/Si/Au = 80/17/3 + PSS) are promising for use in self-cooling devices. We have demonstrated that using sample (iii) with the self-cooling device effectively cools a commercial power MOSFET by the Peltier effect.

#### ACKNOWLEDGEMENTS

The Hall-effect measurement system, scanning electron microscope, and electron-probe micro-analyzer at the Instrumental Analysis Center in Yokohama National University were used. The thermal conductivity and the thermal expansion measurements were carried out in the AGNE Technical Center.

#### REFERENCES

1. S. Yamaguchi, *ULVAC* 52, 14 (2007).
2. S. Fukuda, T. Kato, Y. Okamoto, H. Kitagawa, M. Hamabe, and S. Yamaguchi, *Proceedings of the 26th International Conference on Thermoelectrics* (2007), p. 275.
3. Y. Okamoto, A. Aruga, H. Kasai, J. Morimoto, T. Miyakawa, and S. Fujimoto, *Proceedings of the 13th International Conference on Thermoelectrics* (1994), p. 92.
4. K. Koumoto, M. Shimohigoshi, S. Takeda, and H. Yanagida, *J. Mater. Sci. Lett.* 6, 1453 (1987). doi:10.1007/BF01689320.
5. W.S. Seo, K. Watari, and K. Koumoto, *Proceedings of the 12th International Conference on Thermoelectrics* (1993), p. 175.
6. L.L. Snead, T. Nozawa, Y. Katoh, T.S. Byun, S. Kondo, and D.A. Petty, *J. Nucl. Mater.* 371, 329 (2007). doi:10.1016/j.jnucmat.2007.05.016.
7. M.S. Miao and W.L. Lambrecht, *Phys. Rev. B* 68, 125204 (2003). doi:10.1103/PhysRevB.68.125204.
8. K. Irmischer, *Mater. Sci. Eng. B* 91–92, 358 (2002). doi:10.1016/S0921-5107(01)01071-6.